Proc. NIPR Symp. Antarct. Meteorites, **8**, 79–96, 1995

Ca-Al-RICH INCLUSIONS IN THREE ANTARCTIC CO3 CHONDRITES, YAMATO-81020, YAMATO-82050 AND YAMATO-790992: RECORD OF LOW-TEMPERATURE ALTERATION

Tomoko KOJIMA*, Satomi YADA and Kazushige TOMEOKA

Department of Earth and Planetary Sciences, Faculty of Science, Kobe University, Nada-ku, Kobe 657

Abstract: Ca-Al-rich inclusions (CAIs) in three Antarctic CO chondrites, Yamato (Y)-81020, Y-82050 and Y-790992 have similar overall textures; most CAIs are rimmed or concentric objects. However, there are considerable differences in mineralogy; almost all of the CAIs in Y-81020 consist of primary high-temperature phases such as melilite, anorthite, fassaite and spinel, while most of the CAIs in Y-82050 and Y-790992 contain major amounts of nepheline and lesser amounts of melilite and anorthite. CAIs in Y-790992 contain more nepheline than those in Y-82050. Small grains (<1 μm in diameter) of troilite commonly coexist with nepheline. Spinel in Y-81020 is almost free of Fe, while those in Y-82050 and Y-790992 contain variable amounts of Fe (6 to 60 and 42 to 65 $FeAl_2O_4$ mol%, respectively). The texture of CAIs suggests that nepheline and troilite are secondary alteration products formed by replacing mainly melilite and anorthite. Spinel in CAIs and olivine in amoeboid olivine aggregates probably became enriched in Fe along with the alteration. As the alteration proceeded, fassaite and spinel were also replaced by nepheline, and perovskite was replaced by ilmenite and ulvöspinel. Diopside remained unaltered even in the most heavily altered inclusions. Comparison of mineralogy before and after the alteration suggests that considerable amounts of Na, Fe, S and Cl were introduced into CAIs and some amounts of Ca and Mg were lost. Based on the amounts of nepheline, the relative degrees of alteration of CAIs are as follows: Y-81020<Y-82050<Y-790992.

In order to compare the relationship between alteration of CAIs and thermal metamorphism on the parent body, metamorphic grades of the three CO chondrites were petrographically determined. The results indicate that the metamorphic grade increases in the same order as that of the degree of alteration of CAIs, *i.e.* Y-81020<Y-82050<Y-790992. Therefore, the results raise the possibility that alteration of CAIs may be related to thermal metamorphism which occurred on the meteorite parent body, although further investigation is still needed to verify this hypothesis.

1. Introduction

Ca-Al-rich inclusions (CAIs) in CO carbonaceous chondrites are abundant but generally much smaller than those in CV chondrites. The most common types of inclusions are melilite-rich Type A inclusions and "nodular" spinel-pyroxene aggregates (*e.g.*, MACPHERSON *et al.*, 1988). Besides the primary high-temperature phases, CAIs in some CO chondrites, like those in some CV chondrites, are known to

*Also Mineralogical Institute, Faculty of Science, University of Tokyo, Hongo, Bunkyo-ku, Tokyo 113.

contain variable amounts of relatively low-temperature phases such as nepheline and sodalite (KURAT, 1975; METHOT *et al.*, 1975; IKEDA, 1982; DAVIS, 1985). TOMEOKA *et al.* (1992) showed that CAIs in the Yamato (Y)-791717 CO chondrite contain 5 to 80 vol% of nepheline, and thus are among the most nepheline-rich CAIs known. Most previous workers have interpreted nepheline and sodalite in CAIs as secondary alteration products, and believe that the alteration occurred by reaction with the solar nebula before accretion of CAIs into the meteorites (MACPHERSON *et al.*, 1981; WARK, 1981; HASHIMOTO and GROSSMAN, 1987; HASHIMOTO, 1991). However, GREENWOOD *et al.* (1992) recently pointed out that alteration of CAIs appears to be related to thermal metamorphism of the host meteorites, and thus suggested that alteration of CAIs in CO chondrites may have occurred on the meteorite parent body.

We present here the results of our petrographic and scanning electron microscope studies of CAIs in three Antarctic CO chondrites, Y-81020, Y-82050 and Y-790992. Our study reveals that CAIs in these three meteorites are similar in texture, but differ considerably in mineralogy. In particular, there are large differences in abundance of nepheline; CAIs in Y-81020 are almost free of nepheline, while those in Y-790992 contain major amounts (up to 80 vol%) of nepheline, being equivalent in amount of nepheline to the CAIs in Y-791717; the abundance of nepheline in Y-82050 CAIs is intermediate between these two meteorites. We observed abundant evidence suggesting that nepheline was formed by alteration of the primary high-temperature phases such as melilite and anorthite. Thus the differences in amount of nepheline probably reflect differences in degree of alteration. Therefore, in order to evaluate the hypothesis proposed by GREENWOOD *et al.* (1992), we tried to petrographically determine metamorphic grades of the host meteorites and thereby to compare the degrees of alteration of CAIs and the metamorphic grades.

2. Materials and Methods

Polished thin sections of Y-81020, Y-82050 and Y-790992 were used in this study. CAIs within a total area of ~25 mm^2 in each thin section were examined using an optical microscope and a scanning electron microscope (JEOL JSM 840) equipped with an energy-dispersive X-ray spectrometer (EDS). EDS analyses were obtained at 15 kV and 1.2 nA with a focused beam ~2 μm in diameter. Natural and synthetic minerals were used as standards, and corrections were made by the ZAF method. Accuracy of the EDS analysis was checked by comparison with data by EPMA for the same materials, and the results agreed well as to elements present in more than 1.0 wt%. In order to estimate the metamorphic grade, more than 50 randomly selected olivine grains from Type IA and Type II chondrules, more than 10 kamacite grains, and more than 20 points in the matrix in each meteorite were analyzed with the EDS. For the analysis of the fine-grained matrix, we used a defocused electron beam 25 to 50 μm in diameter.

3. Results

3.1. *Texture and mineralogy*

All of the three CO chondrites contain abundant round to irregularly shaped inclusions; we observed 37, 41 and 30 inclusions in Y-81020, Y-82050 and Y-790992, respectively, each in the area of ~25 mm^2. In each meteorite, most inclusions range in diameter from 50 to 300 μm. Inclusions larger than 300 μm up to 680 μm in diameter sparsely occur in Y-81020 and Y-82050 (six and two inclusions, respectively), while they are absent in Y-790992. Many of the inclusions smaller than 100 μm in diameter are apparently fragments of larger ones. Textures and mineralogy of inclusions are described below in detail.

3.1.1. Y-81020

Among the 37 inclusions studied, 20 inclusions are rimmed objects, which probably correspond to the rimmed "complex" (Type 3) inclusions described by Kornacki and Wood (1984) from the Allende CV3 chondrite. Ten of the rimmed

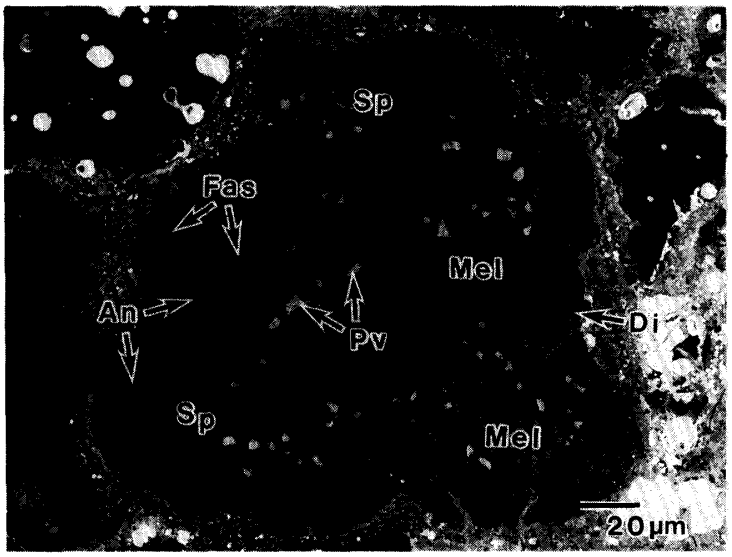

Fig. 1. Back-scattered electron (BSE) image of Y20–41, a typical rimmed inclusion in Y-81020. Its internal area consists of melilite (Mel), spinel (Sp) and perovskite (Pv), surrounded by a layered rim of anorthite (An), fassaite (Fas) and diopside (Di).

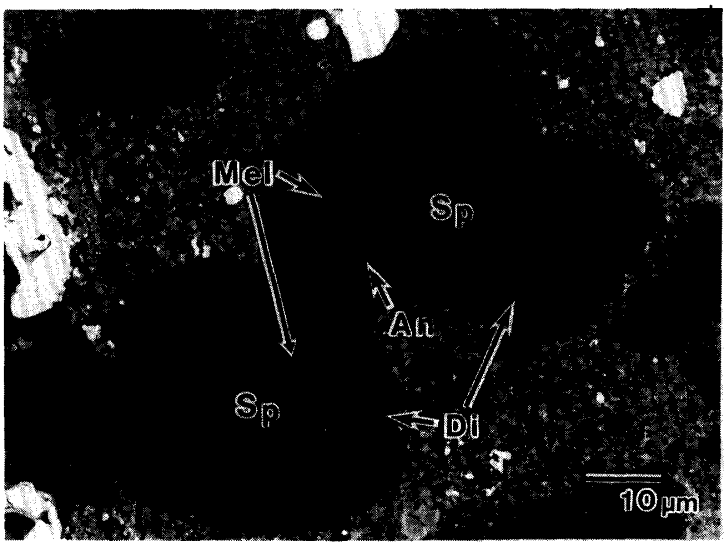

Fig. 2. BSE image of Y20–16, a pair of concentric objects in Y-81020. Each concentric object has a core of spinel mantled by melilite and diopside. Anorthite occurs in minor amount just inside the diopside rim.

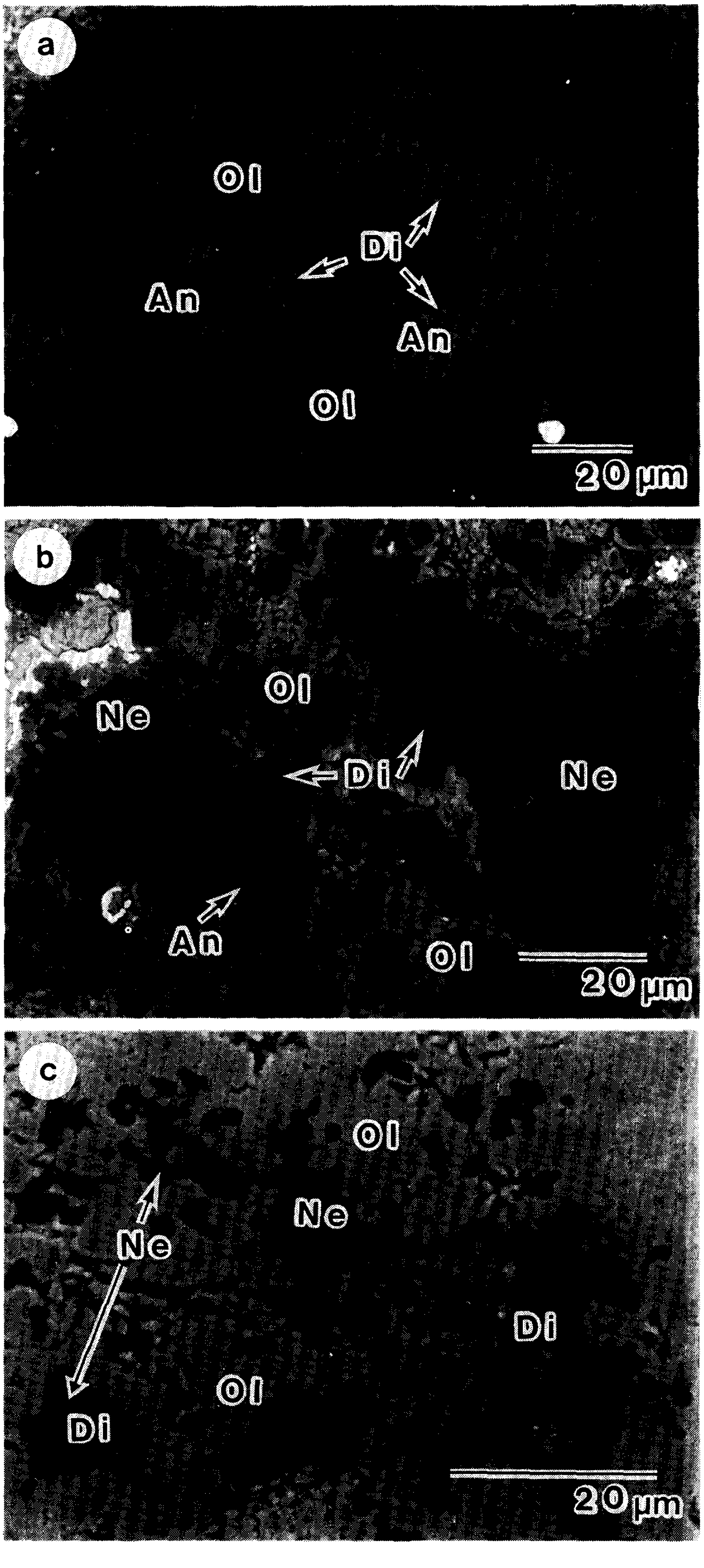

Fig. 3. BSE images of portions of AOAs in Y-81020 (a), Y-82050 (b) and Y-790992 (c). In Y-81020, anorthite occurs in major amounts, while in Y-82050 and Y-790992, it occurs in minor amounts, and instead, nepheline is abundant. Olivine (Ol) in the Y-81020 AOA is nearly free of Fe, while that in the Y-82050 AOA shows strong Fe-Mg zoning, and that in the Y-790992 AOA is Fe rich and homogeneous.

objects have internal areas composed mainly of melilite and spinel enclosing small grains (typically 5 to 10 μm in diameter) of perovskite (Fig. 1). The rims (several to 20 μm in thickness) consist of pyroxene which grades outward from fassaite to diopside. Anorthite occasionally occurs just inside the pyroxene rims. The rest of the rimmed objects have concentric textures and commonly occur as aggregates; each concentric object has a core of spinel with or without perovskite, mantled by melilite and diopside (Fig. 2). They appear to resemble the "nodular" and "banded" spinel-rich inclusions described by MacPherson *et al.* (1983) from the Murchison CM2 chondrite.

Ten inclusions are amoeboid olivine aggregates (AOAs) containing abundant anorthite, fassaite and diopside (Fig 3a). Anorthite grains (mostly 10 to 20 μm in diameter) are surrounded by thin rims (<5 μm in thickness) of fassaite and diopside. Olivine is nearly free of Fe (>Fo_{99}). One AOA contains an unusual Ca-rich phase, probably calcite. Calcite has not been reported from CAIs in CO chondrites. This phase may be a by-product of alteration, but we cannot preclude the possibility that it is a terrestrial weathering product.

Among the remaining CAIs, four inclusions are composed mainly of anorthite, fassaite and diopside. Unlike the CAIs described above, these anorthite-pyroxene inclusions lack rims. Two of the remaining CAIs have cores of $CaAl_4O_7$ enclosing small grains (<5 μm in diameter) of perovskite, surrounded by melilite (Fig. 4). The $CaAl_4O_7$ phase has been identified in CAIs in several carbonaceous chondrites, and is now called grossite (Weber and Bischoff, 1994). An unidentified Na-Al-Fe-rich material (~5.8 wt% Na_2O, ~60 wt% Al_2O_3, ~30 wt% FeO) occurs in these grossite-bearing inclusions. The last CAI is a spherule consisting of fassaite and hibonite.

Representative compositions of constituent minerals are listed in Table 1. In all inclusions, spinel is nearly free of Fe (<1.0 mol% $FeAl_2O_4$), and melilite is mostly gehlenitic (Ge_{85-99}). Fassaite contains 8 to 30 wt% Al_2O_3 and 1 to 14 wt% TiO_2. Anorthite contains <0.1 wt% Na_2O. Diopside in most CAIs contains <3 wt% Al_2O_3, but diopside in AOAs is more aluminous (~7.8 wt% Al_2O_3).

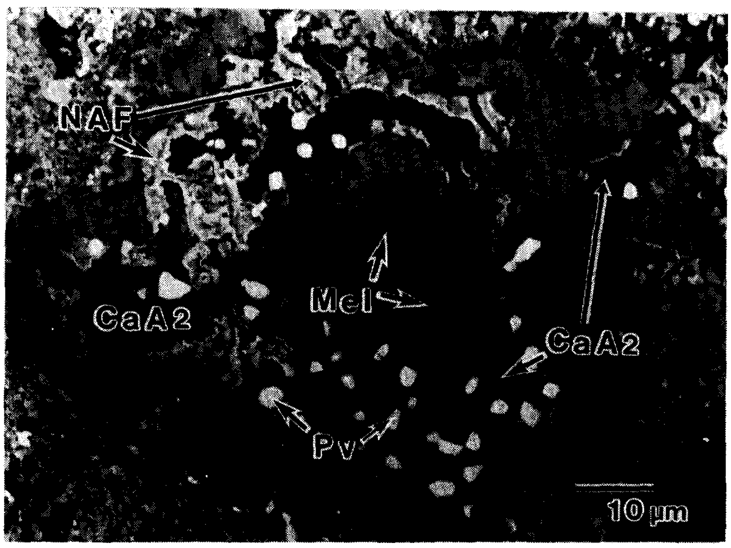

Fig. 4. BSE image of Y20-22, a grossite-bearing, melilite-rich inclusion in Y-81020. Grossite (CaA2) encloses perovskite grains and is surrounded by melilite. A Na-Al-Fe-rich material (NAF) occurs in the upper left portion.

Table 1. EDS analyses of minerals from CAIs in Y-81020.

	Mel	Mel	Sp	Sp	Fas	An	Di
SiO_2	23.2	21.8	0.82	0.17	40.5	42.7	53.5
Al_2O_3	34.2	34.3	70.4	72.5	16.9	33.9	0.86
TiO_2	0.17	0.19	1.01	0.31	4.94	0.21	0.17
FeO	0.50	0.40	0.25	0.36	0.54	0.49	0.65
MgO	1.22	1.31	27.4	27.4	11.8	1.34	19.0
CaO	40.7	40.8	0.97	0.15	24.5	20.8	24.7
Na_2O	0.06	0.04	0.22	0.07	0.05	0.06	0.03
K_2O	0.03	n.d.	0.04	n.d.	n.d.	0.04	n.d.
Cr_2O_3	0.22	0.14	0.26	0.32	0.27	0.21	0.29
NiO	0.45	0.58	0.45	0.43	0.41	0.52	0.30
Total	100.8	99.6	101.8	101.7	99.9	100.3	99.5

Mel=melilite, Sp=spinel, Fas=fassaite, An=anorthite, Di=diopside. n.d.=below detection limit.

3.1.2. Y-82050

Among the 41 inclusions studied, 28 inclusions are rimmed objects similar in texture to those in Y-81020. However, there are important differences in mineralogy; the interiors of the Y-82050 inclusions contain various amounts (mostly <5 to 60 vol%) of nepheline besides spinel, melilite, fassaite and anorthite (Fig. 5). Minor amounts of perovskite also occur in the cores of the inclusions. Small quantities of Cl are detected in nepheline, suggesting that minor amounts of sodalite are intermixed with nepheline. Nepheline commonly forms porous aggregates with fine grains of troilite (mostly <1 μm in diameter). Such a nepheline-troilite association was also found in CAIs in Y-791717 (Fig. in TOMEOKA *et al.*, 1992). Nepheline and troilite commonly have irregular contacts with melilite, anorthite and fassaite, suggesting that they were formed by replacing these primary phases. There is a general tendency for larger inclusions to contain less volume percent of nepheline.

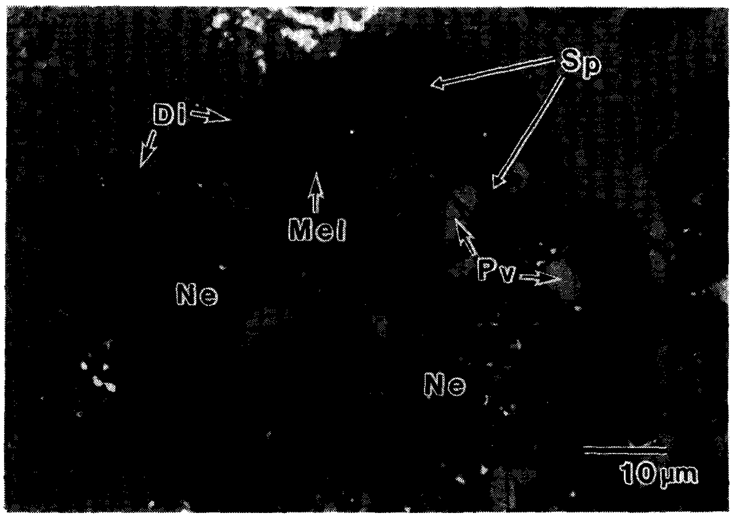

Fig. 5. BSE image of a portion of Y50–2, a rimmed inclusion in Y-82050. It contains a major amount of nepheline (Ne). Tiny bright grains in the nepheline area are troilite.

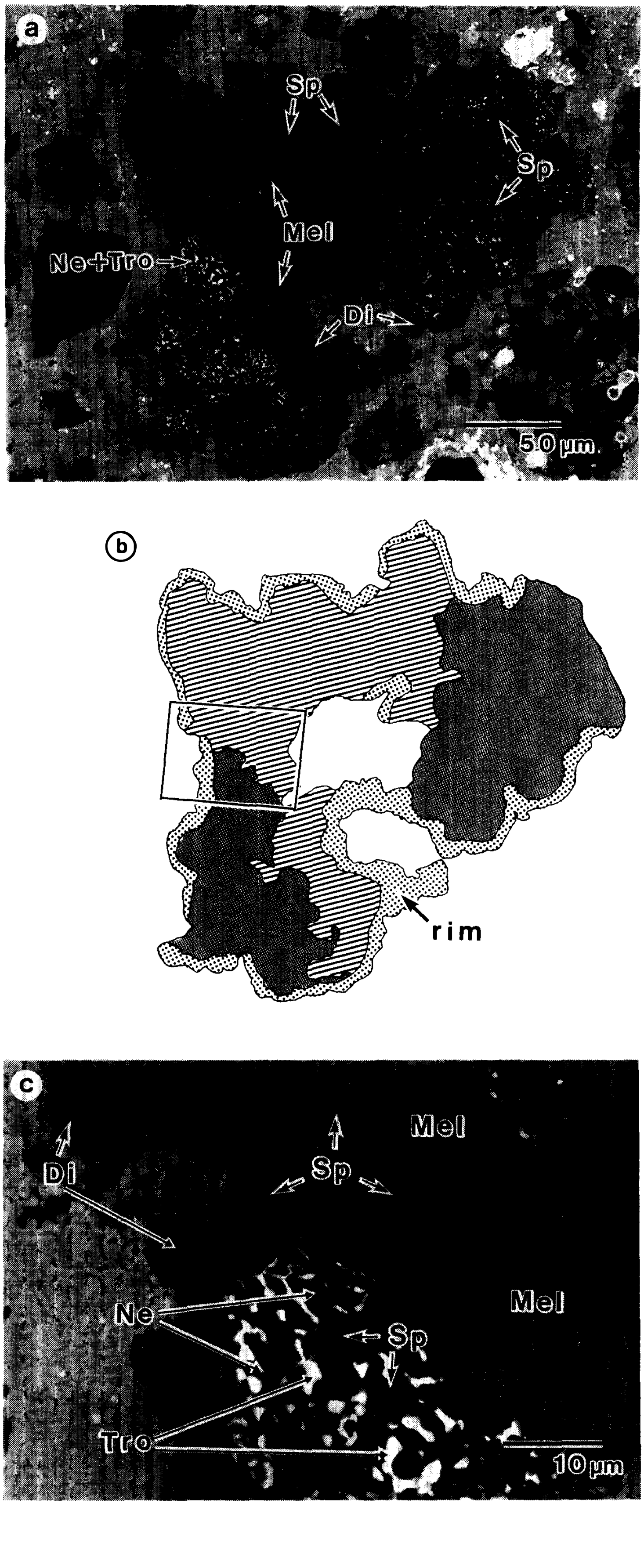

Fig. 6. (a) BSE image of Y50–9, an inclusion composed of melilite-rich and nepheline-rich areas in Y-82050. The inclusion in enclosed by a 5-to-20-μm thick diopside rim except the upper right portion. Spinel in the melilite-rich areas is Fe poor, thus dark in color, while that in the nepheline-rich areas is Fe rich, thus bright. Tiny grains of troilite (Tro: very bright) occur together with nepheline. (b) Illustration showing the melilite-rich areas (hatched areas), the nepheline-rich areas (gray areas) and the rim. (c) Enlarged image of the boxed area in (b), a portion of the boundary between the melilite-rich (upper) and the nepheline-rich (lower) areas.

Five of the rimmed CAIs are relatively large (200 to 280 μm in diameter) and show textures somewhat different from the others (Figs. 6a, b); in each inclusion, 60 to 80 vol% of the internal area is composed mainly of interlocking melilite and spinel, while the remainder is composed mainly of nepheline, troilite and spinel. In the nepheline-rich areas, spinel is distinctly richer in Fe (>20 mol% $FeAl_2O_4$) than that in the melilite-rich areas (<10 mol% $FeAl_2O_4$) and commonly shows Fe-Mg zoning (20 to 50 mol% $FeAl_2O_4$). In the nepheline-rich areas, spinel remains unreplaced, while melilite is replaced by nepheline (Figs. 6a, c). These five inclusions closely resemble the unique melilite-spinel-nepheline-rich inclusion reported from the Y-791717 CO chondrite (Fig. 4 in Tomeoka *et al.*, 1992).

Six AOAs contain nepheline as well as fassaite and diopside (Fig. 3b). Anorthite occurs but in much less amounts than in the Y-81020 AOAs. Olivine in the Y-82050 AOAs is distinctly richer in Fe (Fo_{97-55}) than that in the Y-81020 AOAs and commonly shows strong Fe-Mg zoning. Among other CAIs, three are texturally similar to the anorthite-pyroxene inclusions in Y-81020, but they contain little anorthite but instead abundant nepheline. The rest of the CAIs (three) are aggregates of fine grains of Na-, Al- and Ca-rich material, probably intimate mixtures of nepheline and primary phases.

Representative compositions of constituent minerals are listed in Table 2. Melilite, fassaite and diopside have compositions comparable to those in CAIs in Y-81020. However, spinel is distinctly richer in Fe (6 to 60 mol% $FeAl_2O_4$). Minor amounts of Ca (<3.1 wt% CaO) and Fe (<1.3 wt% FeO) are detected from nepheline; they may come from intimately mixed phases such as melilite, fassaite and troilite. One grain of ilmenite was found to coexist with perovskite in a CAI. Another minor phase is Fe-rich monticellite ($Fe_{0.7}Mg_{0.3}CaSiO_4$), whose composition is comparable to that previously reported from the Felix CO (3.2) chondrite (Greenwood *et al.*, 1992).

3.1.3. Y-790992

Among the 30 inclusions studied, 22 inclusions are rimmed objects texturally similar to those in Y-81020 and Y-82050; eight inclusions among them have concentric textures with spinel cores (Figs. 7a, b). They contain much higher amounts of nepheline (10 to 80 vol%) than those in Y-82050 (Fig. 8). The internal areas of most of the inclusions consist mainly of nepheline, troilite and Fe-rich spinel (45 to 65 mol% $FeAl_2O_4$) with minor fassaite, perovskite and/or ilmenite (Figs. 8 and 9). Melilite and anorthite occur but are rare. Spinel commonly has irregular contacts with nepheline, suggesting that even spinel was replaced by nepheline. Many perovskite grains (<10 μm in diameter) are surrounded by ilmenite rims (Fig. 9). Minor amounts of ulvöspinel (Fe_2TiO_4) also occur together with perovskite. The textural and mineralogical features of the CAIs in Y-790992 most resemble those in the Y-791717 CO chondrite (Tomeoka *et al.*, 1992) among the three meteorites.

Five AOAs also contain large amounts of nepheline (Fig. 3c). Olivine in the AOAs is more Fe rich (Fo_{70-50}) than that in the Y-82050 AOAs and, unlike the latter, shows no zoning. The rest of the CAIs (three inclusions) have textures similar to the anorthite-pyroxene inclusions in Y-81020. However, they contain little anorthite but abundant nepheline like the counterparts in Y-82050.

Table 2. EDS analyses of minerals from CAIs in Y-82050.

	Mel	Sp	Sp	Fas	An	Di	Neph	Neph
SiO_2	23.1	0.26	n.d.	44.6	40.3	53.1	43.0	41.6
Al_2O	33.7	67.0	63.9	12.6	35.6	1.51	37.3	36.0
TiO_2	0.15	0.51	0.32	3.19	0.20	0.19	0.15	0.09
FeO	0.45	7.15	24.8	0.85	1.00	0.49	0.44	0.57
MgO	1.28	22.8	10.6	12.5	0.33	17.3	n.d.	n.d.
CaO	41.1	0.29	0.08	25.2	21.0	26.2	2.25	3.11
Na_2O	0.12	0.08	0.19	0.10	0.44	0.08	17.8	16.7
K_2O	0.07	0.04	0.06	0.05	0.06	0.08	n.d.	0.12
Cr_2O_3	0.18	0.28	0.30	0.33	0.25	0.49	0.44	0.11
NiO	0.61	0.78	0.57	0.43	0.69	0.47	0.41	0.37
Total	100.8	99.2	100.8	99.9	99.9	99.9	101.8	98.7

Neph=nepheline. Other abbreviations as used in Table 1.

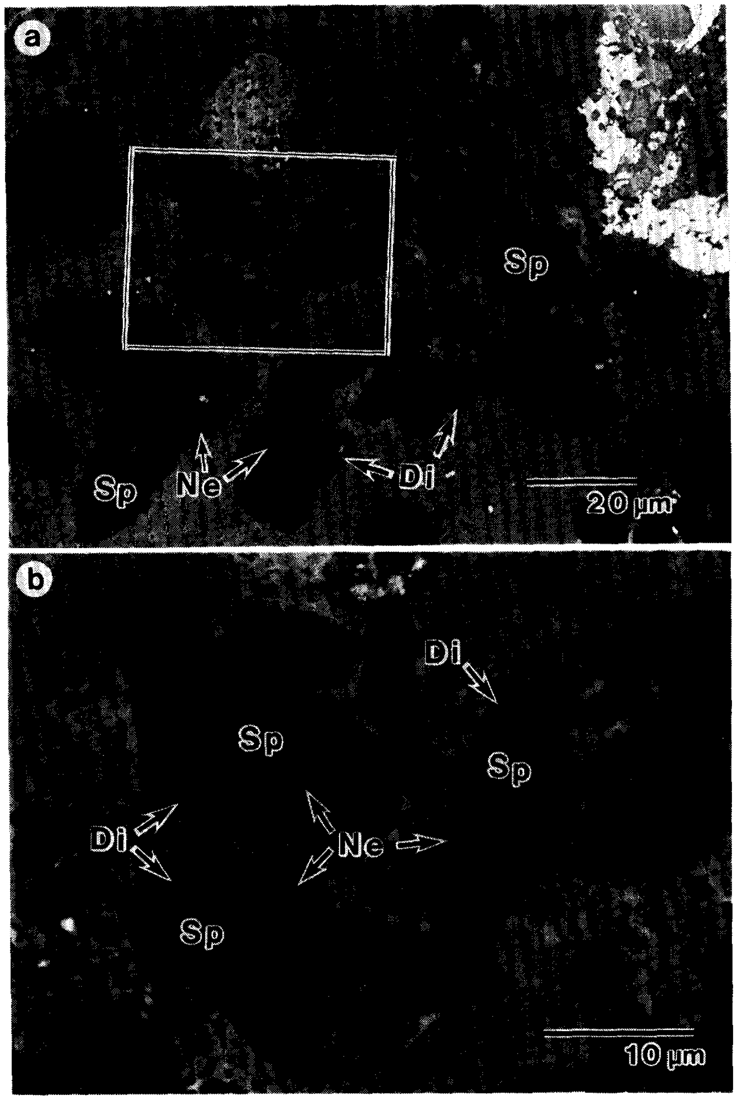

Fig. 7. (a) BSE image of Y992–31, a cluster of concentric objects in Y-790992. The core of each object is composed of Fe-rich spinel surrounded by a nepheline and diopside rim. (b) Enlarged image of the boxed area in (a). Compare their mineralogy and textures with those of Y20–16 in Fig. 2.

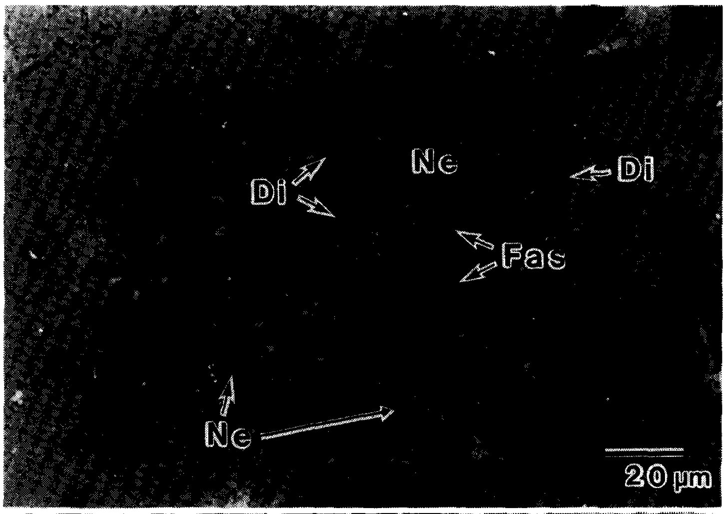

Fig. 8. BSE image of Y992–16, a heavily-altered, rimmed inclusion in Y-790992. Its internal area is composed largely of nepheline with minor fassaite. Diopside rims remain unaltered.

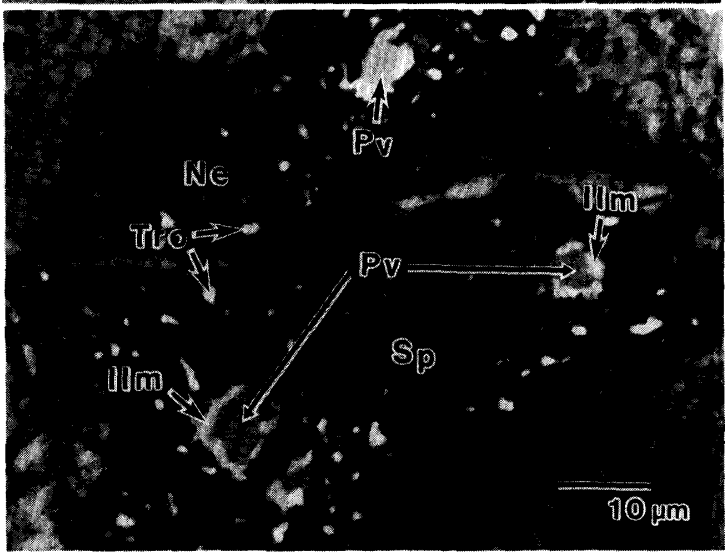

Fig. 9. BSE image of a portion of Y992–23, a heavily-altered inclusion in Y-790992. Perovskite grains are partly replaced by ilmenite (Ilm).

Table 3. EDS analyses of minerals from CAIs in Y-790992.

	Sp	Sp	Fas	Di	Di	Neph	Neph
SiO_2	0.14	0.39	38.0	53.8	49.4	42.4	42.6
Al_2O_3	63.8	63.4	20.9	0.99	7.87	36.9	35.2
TiO_2	0.41	0.20	4.53	0.16	0.80	0.16	0.39
FeO	23.6	23.0	1.28	0.76	0.81	0.56	0.52
MgO	11.1	11.6	10.3	18.4	16.0	0.04	0.62
CaO	0.19	0.32	24.2	25.5	24.9	2.20	2.17
Na_2O	0.21	0.10	0.08	0.06	0.15	18.1	18.3
K_2O	0.04	0.06	n.d.	n.d.	n.d.	0.07	0.03
Cr_2O_3	0.44	0.48	0.26	0.23	0.17	0.22	0.17
NiO	0.46	0.41	0.58	0.28	0.34	0.38	0.24
Total	100.4	100.0	100.1	100.2	100.4	100.9	100.2

Abbreviations as used previously.

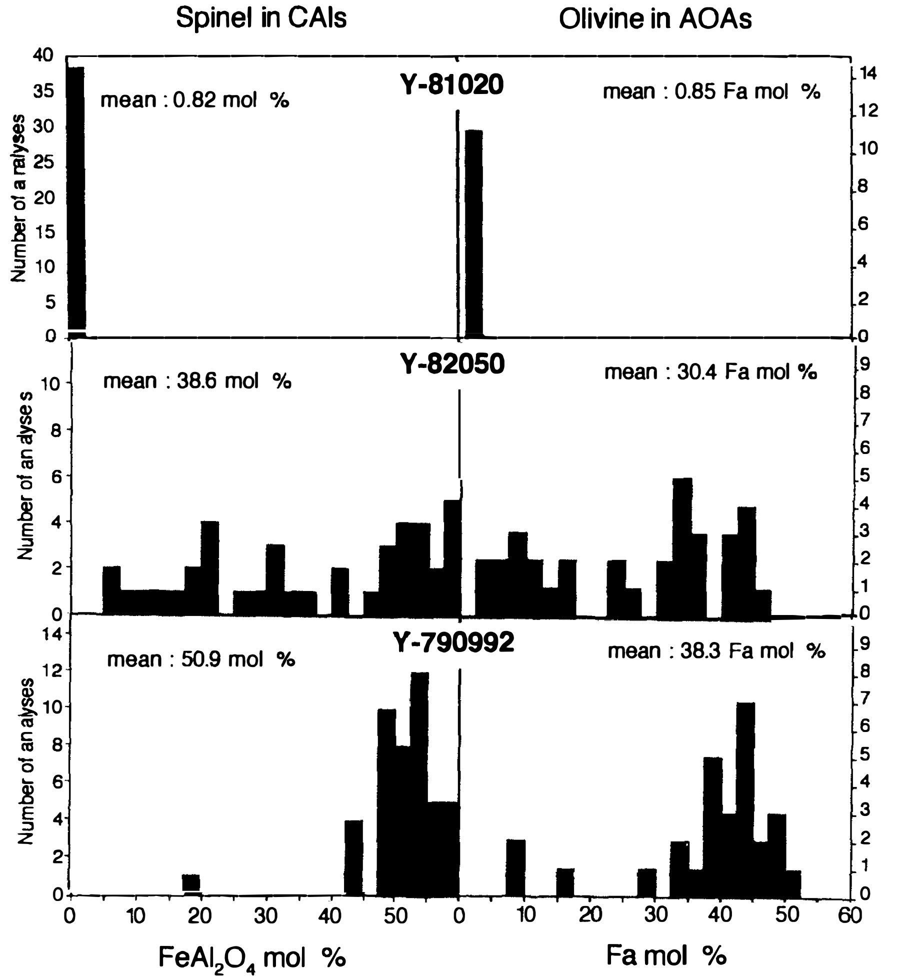

Fig. 10. Histograms of EDS analyses of spinel in CAIs and olivine in AOAs in Y-81020, Y-82050 and Y-790992. Mean Fe contents of spinel and olivine in each meteorite are also shown.

Representative compositions of constituent minerals are listed in Table 3. Fe contents of spinel are higher and narrower in range (mostly 42 to 60 mol% $FeAl_2O_4$) than those in Y-82050 (Fig. 10). Fassaite is richer in Fe (~2.7 wt% FeO), and diopside is richer in Al (~7.9 wt% Al_2O_3) than the counterparts in the CAIs in the other two meteorites. An unidentified Fe-Si-S-rich material (55 to 60 wt% FeO, ~10 wt% SiO_2, 3>wt% S) having fibrous texture is found in several inclusions. This material also occurs in chondrules and the matrix, so it may be a product of terrestrial weathering.

3.2. *Metamorphic grade*

CO3 carbonaceous chondrites are known to comprise a metamorphic sequence, like type 3 ordinary chondrites, that reflects different degrees of thermal metamorphism on their parent bodies. Classification schemes to subdivide CO3 chondrites have been proposed based on petrography (McSween, 1977; Scott and Jones, 1990) and thermoluminescence (TL) sensitivity (Keck and Sears, 1987; Sears *et al.*, 1991).

Table 4. Metamorphic grades of Y-81020, Y-82050 and Y-790992.

	Bulk olivine		Type IA	Type II	Matrix	Kamacite		#TL
	*Fa (mol%)	*σ/Fa (%)	*Fa (mol%)	*CaO (wt%)	FeO/(FeO+MgO)	Ni	Cr	sensitivity
Y-81020	10.1	138	1.34	0.27	0.78	5.75	0.49	0.07±0.02
	3.0	*3.0*	*3.0*	*3.0*	*3.0*	*3.7*	*3.1*	*3.3*
Y-82050	15.4	111	6.38	0.22	0.71	5.30	0.48	0.054±0.008
	3.1	*3.1*	*3.3*	*3.1*	*3.2*	*3.5*	*3.1*	*3.3*
Y-790992	18.4	70	14.2	0.16	0.72	5.27	0.35	—
	3.3	*3.5*	*3.5*	*3.4*	*3.2*	*3.5*	*3.2*	

Italicized figures are petrologic types defined based on Table 8 in SCOTT and JONES (1990) (parameters marked by *) and on Table 3 in SEARS *et al.* (1991).
#Data from SEARS *et al.* (1991).

Y-81020 and Y-82050 have been previously classified as 3.3 by the TL method (SEARS *et al.*, 1991) (TL data for Y-790992 are currently unavailable). But SCOTT and JONES (1990) suggested that compositions of olivine in chondrules are the most useful diagnostic property in evaluating metamorphic effects. Thus we tried to analyze olivines in chondrules in the three CO chondrites and also to determine other petrographic features diagnostic of metamorphism in the hope of comparing relationships between alteration of CAIs and metamorphic grades of host meteorites. The results are summarized in Table 4.

Table 5. EDS broad beam analyses of matrices of Y-81020, Y-82050 and Y-790992.

	Y-81020		Y-82050		Y-790992	
	Mean	s.d.	Mean	s.d.	Mean	s.d.
SiO_2	22.7	2.8	26.5	2.42	23.1	2.22
Al_2O_3	1.63	0.81	1.58	0.49	1.04	0.32
TiO_2	0.12	0.03	0.15	0.03	0.14	0.04
FeO	39.0	5.54	40.7	2.77	40.5	6.94
MnO	0.38	0.07	0.50	0.07	0.46	0.05
MgO	11.2	1.84	16.6	1.52	15.4	1.58
CaO	0.78	0.45	1.07	0.88	0.36	0.33
Na_2O	n.d.	—	n.d.	—	n.d.	—
K_2O	0.12	0.06	0.04	n.d.	0.04	n.d.
Cr_2O_3	0.39	0.08	0.51	0.11	0.44	0.10
NiO	2.84	0.66	2.39	0.58	2.65	0.7
P_2O_5	0.08	0.05	n.d.	—	0.11	0.07
SO_3	1.73	0.45	0.99	0.79	1.70	0.66
Total	81.0		91.0		85.9	

s.d.=standard deviations.

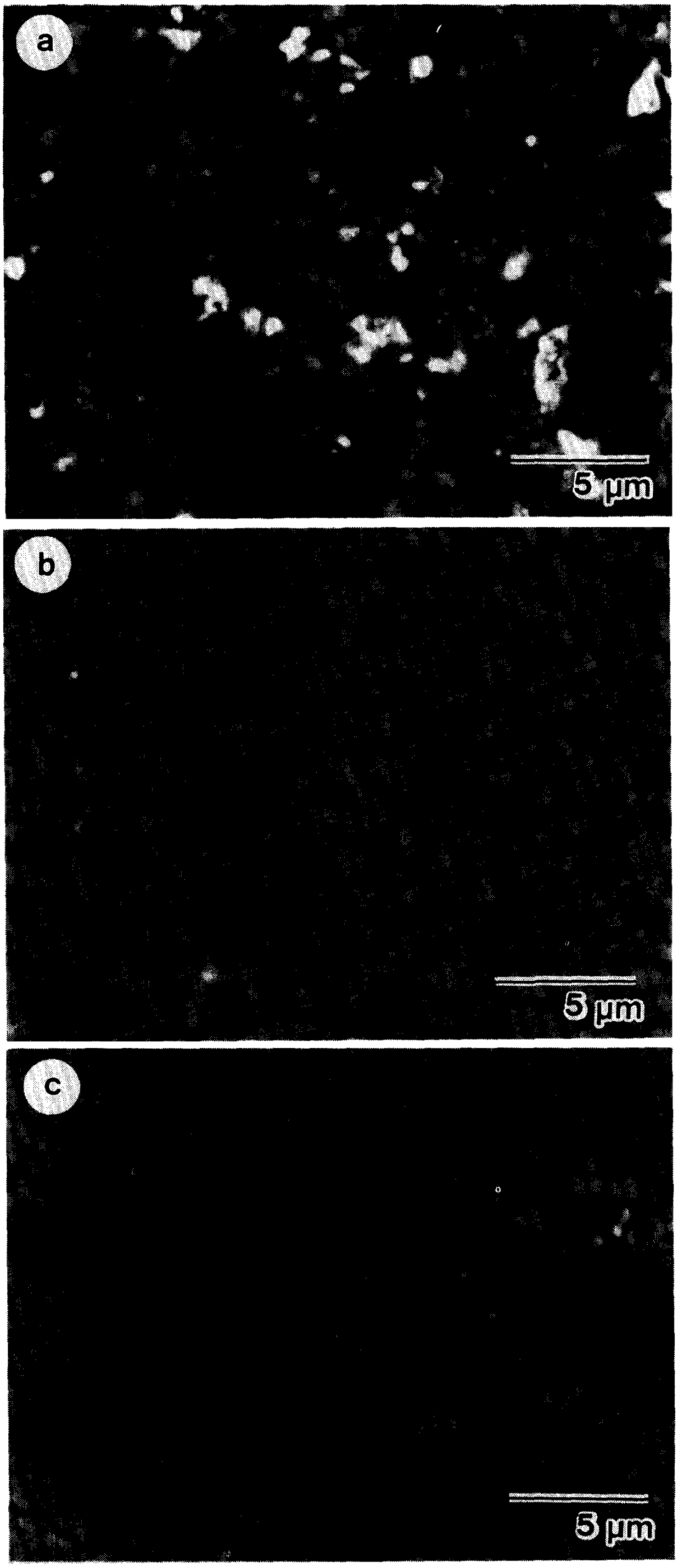

Fig. 11. High-magnification BSE images of the matrices of Y-81020 (a), Y-82050 (b) and Y-790992 (c).

With increasing metamorphism, olivines in chondrules are expected to become richer in Fe, whereas those in the matrix become poorer in Fe (McSWEEN, 1977; SCOTT and JONES, 1990). In Y-81020, olivines in Type IA chondrules are very magnesian (Fo_{99-100}) and homogeneous, whereas in Y-82050 and Y-790992, olivines in Type IA chondrules are distinctly richer in Fe (Fo_{74-99} and Fo_{62-98}, respectively) and commonly show strong Fe-Mg zoning. Based on the olivine compositions, we assign the petrologic subtypes 3.0, 3.1, and 3.3–3.5 to Y-81020, Y-82050 and Y-790992, respectively.

Broad-beam analyses of the matrices in the three CO chondrites are shown in Table 5. The matrix in Y-81020 has a higher average FeO/(FeO+MgO) ratio than those in the other two meteorites (Table 4). The matrix in Y-81020 consists of extremely fine grains and contains numerous grains of Fe-rich phase, probably Fe metal or sulfide (Fig. 11a). The relatively high FeO/(FeO+MgO) ratio and S contents of the Y-81020 matrix are probably due to these grains. The matrices of Y-82050 and Y-790992 consist of coarser grains (1 to 5 μm in diameter) and are chemically more homogeneous than the matrix of Y-81020 (Figs. 11b, c), suggesting that they may have been recrystallized and homogenized. These compositional and textural features of the matrices also support the finding that Y-81020 is lower in metamorphic grade than the other two meteorites.

Compositions of kamacite in chondrules and the matrix are listed in Table 4. With increasing metamorphism, Cr content of kamacite is expected to decrease, while Ni and Co contents increase (McSWEEN, 1977; SCOTT and JONES, 1990; SEARS *et al.*, 1991). Analysis for Co is not available in this study. In Y-81020, kamacite is the most common opaque phase, while in Y-82050 and Y-790992, kamacite is rare, and troilite and taenite are common. In each of the three meteorites, kamacite in chondrules is richer in Cr and poorer in Ni than that in the matrix, being consistent with the finding that metamorphic exchange took place between metals and the matrix (McSWEEN, 1977). Ni contents of kamacite in Y-81020 are apparently higher than those of kamacite in the other two meteorites; this appears to be inconsistent with the finding that Y-81020 is lower in metamorphic grade. However, as discussed in SCOTT and JONES (1990), this may be due to a process other than metamorphism.

4. Discussion

4.1. Comparison of CAIs in three meteorites

Inclusions in the three Antarctic CO chondrites have similar overall textures; most are rimmed objects, some of which have concentric textures (Figs. 2 and 7). However, the mineralogies, particularly of the internal areas, differ considerably between the three meteorites. The internal areas of the rimmed inclusions in Y-81020 are composed mainly of melilite and Mg-rich spinel, while most inclusions in Y-82050 and Y-790992 contain little melilite but abundant nepheline. Inclusions other than the rimmed ones also show similar mineralogical and textural features. The AOAs in Y-82050 and Y-790992 (Figs. 3b, c) contain little or no anorthite, but instead abundant nepheline. The nepheline-pyroxene-rich inclusions in Y-82050 and Y-790992 probably correspond to the anorthite-pyroxene inclusions in Y-81020.

Textures of those inclusions in Y-82050 and Y-790992 suggest that nepheline is a secondary alteration product formed mainly by replacing melilite and anorthite; the nepheline commonly occurs as porous aggregates and shows irregular contact with primary phases (*e.g.*, Figs. 5, 6c). Condensation calculations indicate that nepheline condenses at relatively low temperature ($<$1100 K; FEGLEY and LEWIS, 1980). Therefore, alteration of CAIs presumably occurred at relatively low temperature.

From the textures and mineralogy, it is probably that the inclusions in Y-82050 and Y-790992 were once rich in melilite and anorthite, like those in Y-81020, but during alteration, melilite and anorthite were preferentially consumed to form nepheline. Along with the alteration, spinel and olivine in the inclusions were enriched in Fe. The differences in mineralogy between the inclusions in Y-81020, Y-82050 and Y-790992 probably reflect different degrees of low-temperature alteration. Based on the amounts of nepheline, we deduce that the relative degrees of alteration are as follows: Y-81020 $<$Y-82050 $<$Y-790992. CAIs in another Antarctic CO3 chondrite, Y-791717, are reported to also contain abundant nepheline (TOMEOKA *et al.*, 1992). The occurrence of nepheline in Y-791717 CAIs is similar to that of nepheline in Y-82050 and Y-790992 CAIs, suggesting that CAIs in these three chondrites experienced similar alteration processes. From the amounts of nepheline, the degree of alteration of Y-791717 CAIs appears to be equivalent to that of CAIs in Y-790992.

Although nepheline was not found, CAIs in Y-81020 may not have escaped alteration. Grossite-bearing inclusions are found only in Y-81020, in which the unusual Na-Al-rich material occurs (Fig. 4). From the texture, it is quite possible that the Na-Al-Fe-rich material was formed by replacing grossite. GREENWOOD *et al.* (1993) found that grossite in a CAI from the Vigarano CV3 chondrite is partially replaced by a fibrous material having a composition close to $FeAl_2O_4$, while melilite in the same CAI remains unaltered, suggesting that grossite is even more susceptible to alteration than melilite. This may explain why grossite is absent in Y-82050 and Y-790992. Although the Na-Al-Fe-rich material may have resulted from alteration, the effect of alteration in Y-81020 CAIs was so small that melilite and anorthite remain unaltered.

4.2. *Mineralogical and chemical change during alteration*

Melilite and anorthite are known to be the most susceptible to alteration among the primary phases in CAIs (*e.g.*, BARBER *et al.*, 1984; HASHIMOTO and GROSSMAN, 1987; MACPHERSON *et al.*, 1988; TOMEOKA *et al.*, 1992), which was also confirmed by the present study. As the alteration proceeded, fassaite and even spinel appear to have been subjected to alteration. Perovskite was replaced by ilmenite and ulvöspinel in heavily altered inclusions (Fig. 9). However, diopside remains unaltered even in heavily altered inclusions (Fig. 8), and thus seems to be the most resistant to alteration among the primary phases. The relative degrees of resistance to alteration are probably as follows: (melilite, anorthite)$<$(spinel, perovskite)$<$diopside. The sequence is consistent with the previously reported results on CAIs from CV (HASHIMOTO and GROSSMAN, 1987) and CO (TOMEOKA *et al.*, 1992) chondrites.

During alteration of CAIs, it is evident that considerable chemical changes took place. Troilite is another major phase formed together with nepheline. Spinel and olivine in altered inclusions are commonly enriched in Fe. Mean Fe contents of spinel and olivine increase in the order Y-81020<Y-82050<Y-790992 (Fig. 10). There are also several Fe-rich phases such as ilmenite, ulvöspinel and Fe-rich monticellite which appear to be by-products of alteration. Therefore, considerable amounts of not only Na and Cl, but also Fe and S, were probably introduced into CAIs, and some amounts of Ca and Mg were lost.

4.3. Relationship between alteration of CAIs and metamorphism

It is commonly believed that nepheline and sodalite in CAIs from CV3 and CO3 chondrites were formed by reaction of primary phases with a Na-, Fe- and Cl-rich nebular gas before accretion to the meteorite parent body (*e.g.*, MACPHERSON *et al.*, 1981; WARK, 1981; HASHIMOTO and GROSSMAN, 1987; HASHIMOTO, 1991). However, GREENWOOD *et al.* (1992) recently studied CAIs in four non-Antarctic CO chondrites and suggested that the degree of alteration of CAIs is correlated with the metamorphic grade of the host meteorites, and thus suggested that alteration of CAIs took place on the parent body. Indeed, previous reports of nepheline from CAIs in CO chondrites are from those classified into relatively high metamorphic grades (Lancé (3.3), KURAT, 1975; Isna (3.7), METHOT *et al.*, 1975; ALH-77003 (3.5), IKEDA, 1982; Ornans (3.4), DAVIS *et al.*, 1985).

Based on TL sensitivity measurements (SEARS *et al.*, 1991), Y-81020 and Y-82050 are both classified as metamorphic grade 3.3 (TL data for Y-790992 are currently unavailable). However, our petrographic study shows that there are apparent differences in metamorphic grade among Y-81020, Y-82050 and Y-790992; the data shown in Table 4, except for Ni contents in kamacite, suggest that the metamorphic grade of the three meteorites increases in the order Y-81020<Y-82050<Y-790992. This order is the same as that proposed for the degree of alteration of CAIs, supporting the suggestion of GREENWOOD *et al.* (1992). It seems that the correlation between the degree of alteration of CAIs and the metamorphic grade also holds for Y-791717; olivine in Type IA chondrules in Y-791717 shows strong Fe-Mg zoning suggesting high metamorphic grade for this meteorite.

The FeO/(FeO+MgO) ratio and S contents of the matrix of Y-81020 are higher than those of the matrices of Y-82050 and Y-790992 (Tables 4 and 5). This may suggest that Fe and S might have been redistributed from the matrix to CAIs and AOAs in the latter two meteorites during *in situ* alteration, although the influence of terrestrial weathering cannot be excluded. However, we have not observed any direct evidence that elemental exchange took place between the inclusions and matrix. Therefore, further systematic studies of CAIs as well as the chondrules and matrix in CO chondrites are required to verify whether low-temperature alteration of CAIs took place on the meteorite parent body or not.

Acknowledgments

We thank the National Institute of Polar Research for loaning the thin sections to us. Prof. N. NAKAMURA provided valuable discussion, and Prof. G. KURAT and an anonymous referee provided thoughtful reviews. We also thank Dr. H. MAEKAWA for use of the SEM. Scanning electron microscopy and EDS analyses were performed at the Department of Earth and Planetary Sciences, Kobe University. This work was supported in part by a Grant-in-Aid of the Japan Ministry of Education, Science and Culture (No. 06403001 and 06209207) and by the Hyogo Science and Technology Foundation.

References

BARBER, D. J., MARTIN, P. M. and HUTCHEON, I. D. (1984): The microstructure of minerals in coarse-grained Ca-Al-rich inclusions from the Allende meteorite. Geochim. Cosmochim. Acta, **48**, 769–783.

DAVIS, A. M. (1985): Refractory inclusions in the Ornans C3O chondrite. Lunar and Planetary Science XVI. Houston, Lunar Planet. Inst., 165–166.

FEGLEY, B., Jr. and LEWIS, J. S. (1980): Volatile element chemistry in the solar nebula: Na, K, F, Cl, Br, and P. Icarus, **41**, 439–455.

GREENWOOD, R. C., HUTCHISON, R., HUSS, G. R. and HUTCHEON, I. D. (1992): CAIs in CO3 meteorites: Parent body or nebula alteration? Meteoritics, **27**, 229.

GREENWOOD, R. C., MORSE, A. and LONG, J. V. P. (1993): Petrography, mineralogy and Mg isotope composition of VICTA: A Vigarano $CaAl_4O_7$-bearing Type A inclusion. Lunar and Planetary Science XXIV. Houston, Lunar Planet. Inst., 573–574.

HASHIMOTO, A. (1991): The effect of H_2O gas on volatilities of planet-forming major elements: I. Experimental determination of thermodynamic properties of Ca-, Al-, and Si-hydroxide gas molecules and its application to the solar nebula. Geochim. Cosmochim. Acta, **56**, 511–532.

HASHIMOTO, A. and GROSSMAN, L. (1987): Alteration of Al-rich inclusions inside amoeboid olivine aggregates in the Allende meteorite. Geochim. Cosmochim. Acta, **51**, 1685–1704.

IKEDA, Y. (1982): Petrology of the ALH-77003 chondrite (C3). Mem. Natl Inst. Polar Res. Spec. Issue, **25**, 34–65.

KECK, B. D. and SEARS, D. W. G. (1987): Chemical and physical studies of type 3 chondrites, VIII: The CO chondrites. Geochim. Cosmochim. Acta, **51**, 3013–3022.

KORNACKI, A. and WOOD, J. A. (1984): Petrography and classification of Ca, Al-rich and olivine-rich inclusions in the Allende CV3 chondrite. Proc. Lunar Planet. Sci. Conf., 14th, Pt. 2, B573–B587 (J. Geophys. Res., **89** Suppl.).

KURAT, G. (1975): Der Kohlige Chondrit Lancé: Eine petrologische Analyse der komplexen Genese eines Chondriten. Tschermaks Mineral. Petrogra. Mitt., **22**, 38–78.

MACPHERSON, G. J., GROSSMAN, L., ALLEN, J. M. and BECKETT, J. R. (1981): Origin of rims on coarse-grained inclusions in the Allende meteorite. Proc. Lunar Planet. Sci. Conf., 12B, 1079–1091.

MACPHERSON, G. J., BAR-MATTHEWS, M., TANAKA, T., OLSEN, E. and GROSSMAN, L. (1983): Refractory inclusions in the Murchison meteorite. Geochim. Cosmochim. Acta, **47**, 823–829.

MACPHERSON, G. J., WARK, D. A. and ARMSTRONG, J. T. (1988): Primitive material surviving in chondrites: Refractory inclusions. Meteorites and the Early Solar System, by J. F. KERRIDGE and M. S. MATTHEWS. Tucson, Univ. Arizona Press, 746–807.

MCSWEEN, H. Y. (1977): Carbonaceous chondrites of the Ornans type: A metamorphic sequence. Geochim. Cosmochim. Acta, **41**, 477–491.

METHOT, R. L., NOONAN, A. F., JAROSEWICH, E., DE GASPARIS, A. A. and AL-FAR, D. M. (1975): Mineralogy, petrology and chemistry of the Isna (C3) meteorite. Meteoritics, **10**, 121–131.

SCOTT, E. R. D. and JONES, R. H. (1990): Disentangling nebular and asteroidal features of CO3 carbonaceous chondrites. Geochim. Cosmochim. Acta, **54**, 2485–2502.

SEARS, D. W. G., BATCHELOR, J. D., LU, J. and KECK, B. D. (1991): Metamorphism of CO and CO-like chondrites and comparisons with type 3 ordinary chondrites. Proc. NIPR Symp. Antarct. Meteorites, **4**, 319–343.

TOMEOKA, K., NOMURA, K. and TAKEDA, H. (1992): Na-bearing Ca-Al-rich inclusions in the Yamato-

791717 CO carbonaceous chondrite. Meteoritics, **27**, 136-143.

WARK, D. A. (1981): Alteration and metasomatism of Allende Ca-Al-rich materials. Lunar and Planetary Science XII. Houston, Lunar Planet. Inst., 1145–1147.

WEBER, D. and BISCHOFF, A. (1994): The occurrence of grossite ($CaAl_4O_7$) in chondrites. Geochim. Cosmochim. Acta, **58**, 3855–3877.

(*Received September 12, 1994; Revised manuscript received December 14, 1994*)